# Low Carbon Footprint Hybrid Battery Charger

By: Blake Kennedy, Philip Thomas

Bradley University Department of
Electrical and Computer Engineering

Advisors: Mr. Gutschlag, Dr. Huggins

May 14, 2008

# Abstract

The Low Carbon Footprint Hybrid Battery Charger uses photovoltaic arrays and a wind turbine to charge a stationary battery. The stationary battery is then used to quick-charge a battery for vehicular applications. The project emphasizes efficient energy usage by utilizing switch mode power supply design to minimize power dissipation. Technical topics covered in this paper include battery chemistry, buck-boost design, and lead-acid battery charging techniques.

# Table of Contents

# 1. Introduction

The goal of the Low Carbon Footprint Hybrid Battery Charger project is to charge a battery for vehicular applications using the renewable energy resources of photovoltaic arrays and a wind turbine. The project emphasizes efficient energy usage by utilizing switch mode power supply design to minimize power dissipation. The system's possible modes of operation can provide either maximum battery life, minimum charge time, or emergency charge. The completed system will require:

1. using photovoltaic arrays and a wind turbine as renewable energy sources to charge an electric car battery overnight
2. a power control system that optimizes use of renewable energy
3. a microcontroller based user interface
4. an efficient system for charging a mobile battery from a stationary battery

# 2. Purpose

The primary application of the Low Carbon Footprint Hybrid Battery Charger is for vehicular applications. A system like this would be ideal for any commuter who travels less than about 40 miles (round trip) to work and wants to reduce their carbon emissions or save some money in comparison to using carbon based fuels. The commuter would mount photovoltaic arrays and a wind turbine at their home to continually charge a stationary battery. Whenever their vehicle needs charging, the mobile battery can be charged from the stationary battery.

This project used a scaled down vehicle to demonstrate the theory involved in such a system. The target vehicle is the Gaucho, an electric kid's toy ride on vehicle, which has been used for previous projects at Bradley University. The Gaucho battery has significantly less capacity than what would be required for full scale applications.

# 3. System Description

Figure 1 depicts the high level system block diagram. The dotted lines in the figure represent control signals and the solid lines represent power flow. The control signals will be used to control the flow of power and transmit data for the user interface. Power flow is the path the power will follow through during the charging process to reach the mobile battery.

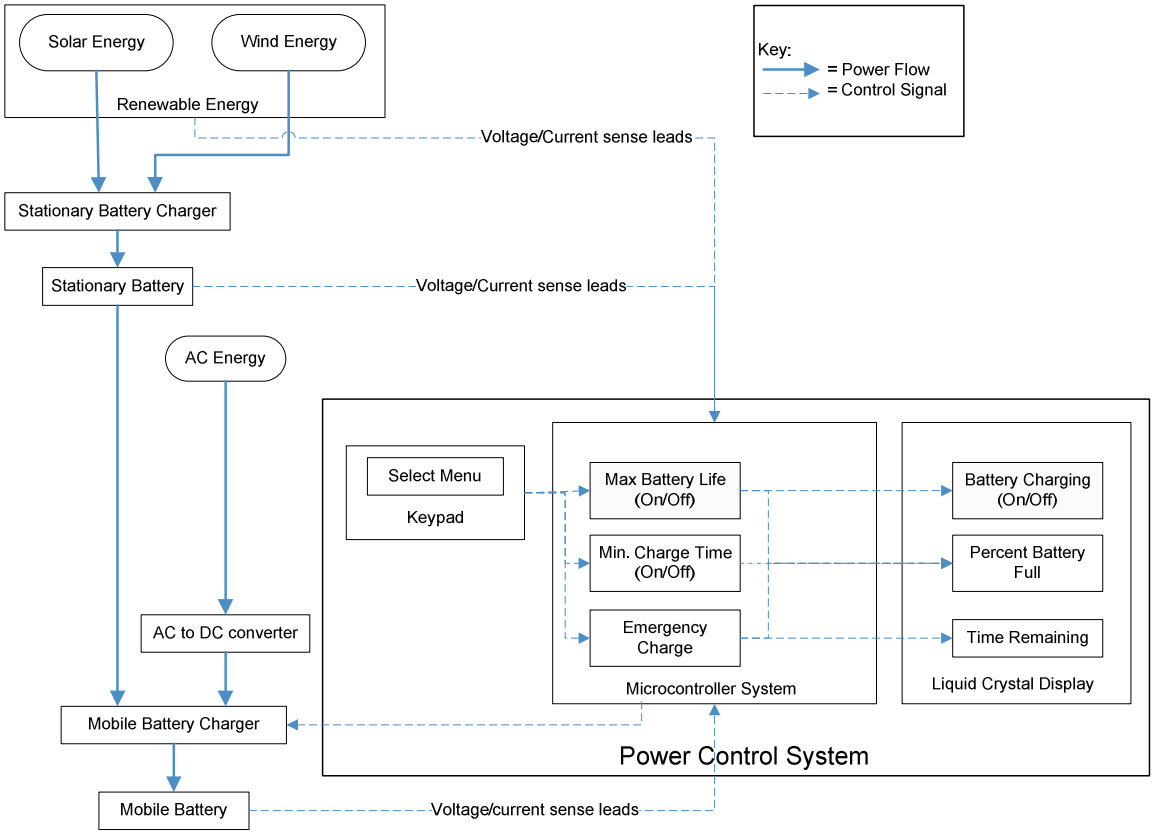


Figure 1: High Level System Block Diagram

Figure 2 shows a more detailed flowchart of the same system. In Figure 2, the two buck-boost components, two switching regulator integrated circuits (IC), two gate drivers, and the lead acid fast charge IC before the stationary battery compose the stationary battery charger block shown in Figure 1. The two buck-boost systems will regulate the voltage of the renewable energy sources so they can easily be combined into one power source. The lead acid fast charge IC is needed to control the battery charging. The same arrangement of blocks containing different components also creates the mobile battery charger. Each subsystem in Figure 2 will be explained in detail.

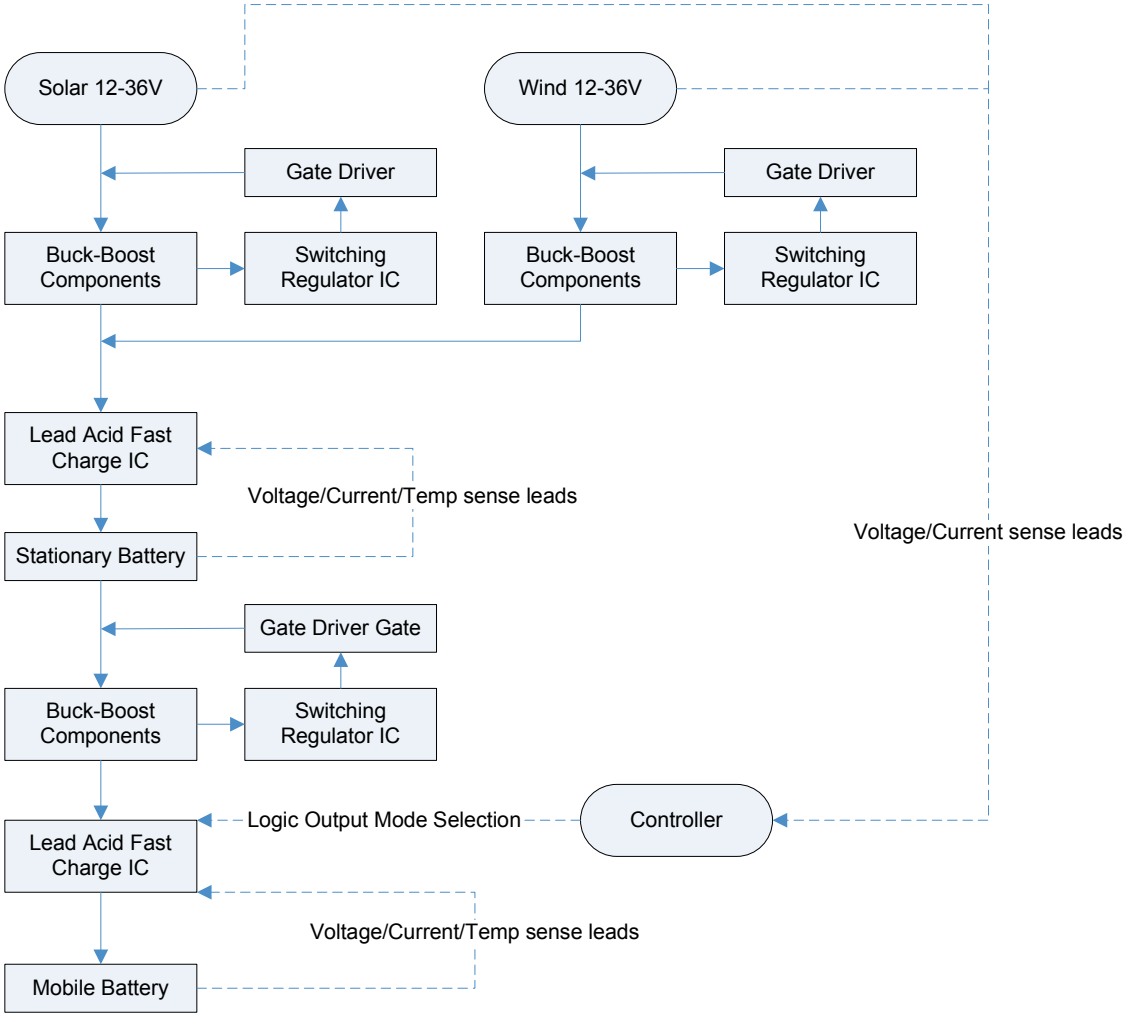


Figure 2: Detailed Flow Chart

## *3.1 Solar Energy*

Two BP350J photovoltaic (PV) arrays were selected to collect solar energy. The maximum specifications for the arrays are 50W, 17.5V, and 2.9A per array. The photovoltaic arrays can provide sufficient energy to charge the mobile battery given 1.470 sun hours (kilowatt*hrs/$m^2$/day) in Peoria, Illinois with 0 M.P.H. winds [1]. Figure A-1 in appendix A shows the Matlab code created to calculate the minimum number of photovoltaic arrays. This code uses sun hours from the Advanced Energy Group [1] shown in Figure 3. The worst case condition for sun hours used was in Chicago, IL. The best case condition for sun hour data was taken in Saint Louis, MO. The average amount of sun hours used in this code represents Peoria, IL. The calculations concluded that two PV arrays would be adequate. The full results of the calculations are shown in Figure A-2 in Appendix A. This code also calculated the efficiency of the BP350J solar panel to be 13.22% based on the characteristics specified in the datasheet.


Figure 3: Midwest Average Low Peak Solar Insolation [2]

The maximum specification for the solar voltage and current (limited by the stationary battery charger input) is 36V at 10A. The maximum output from the PV arrays into the stationary battery charger in a series configuration is within specifications at 17.5V, 5.8A.

## *3.2 Wind Energy*

Ideally, wind energy would be provided by a full scale residential wind turbine. For proof of concept, a DC power supply simulated a scaled down version of a wind turbine. The wind turbine specifications were modeled after the 400W Air-X residential wind turbine. However, it was assumed the output of the turbine was a variable voltage based on the turbine speed to make the system more robust.

The turbine's specifications were compared against the worst case power generation for Peoria, IL. Based on the U.S. Department of Energy's statistics, the average wind speed at a height of 50 meters in Peoria is 14.3-15.7 M.P.H [3]. Based on the Matlab code in Figure A-1, in Appendix A, 1.4 kWh/week (0.2016 kWh/day) are required to provide enough energy to fully charge the mobile battery everyday of the week. The wind turbine specifications indicate that if wind speeds of 12 M.P.H., 1.2kWh/day of energy will be produced [4]. This is ample energy for this application, and within the stationary battery charger input specifications.

### *3.3 Buck-Boost Components*

The basic buck-boost topology is shown in Figure 4. The four major components of the circuit are a switch, inductor, capacitor, and diode. When the switch is closed the inductor charges and the load's energy is provided by the capacitor. When the switch is open, the inductor supplies energy to the load and charges the capacitor. The inductor current must remain above zero (or operating in continuous mode) for the design equations to be accurate. Ideally, a 50% switching duty cycle in continuous mode would result in the output voltage equaling the input voltage. A duty cycle above 50% would result in a boost power supply, and a duty cycle below 50% would result in a buck power supply. The switching speed influences the inductor and capacitor sizes, and a switching frequency of between 20kHz-100kHz is desirable to minimize component sizes. A reduction in inductor size is beneficial in lowering DC copper resistance and thereby increasing efficiency.

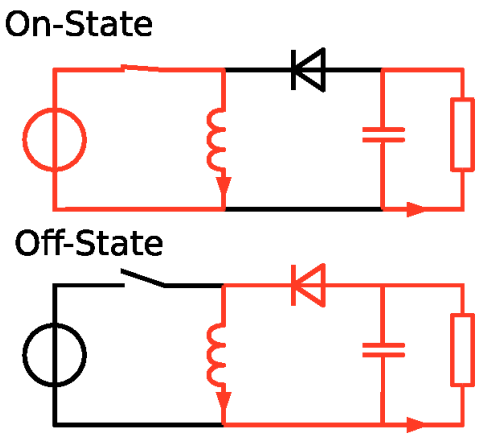

Figure 4: Basic Buck-Boost Topology

Components were selected by first calculating the minimum theoretical values via the Matlab code in Figure A-3, Appendix A. After various specifications for the buck-boost supply were identified, the minimum inductance and capacitance were found from a Texas Instruments buck-boost design reference [5]. The minimum component values calculated are shown in Figure A-4, Appendix A. An inductance of 800μH was used instead of the minimum value calculated to increase the L/R time constant. This was done to prevent the input voltage being from being short circuited during system start-up. A schottky diode was used because of its low forward voltage drop and rapid recovery time. A MOSFET and gate drive circuitry were used as the switch in the circuit.

The specifications for the buck-boost system require converting a varying voltage of 12-36V to 14.2V DC at 10A maximum current. The component parameters must also be operational at the switching frequency of 50kHz. The Switching Regulator IC and Gate Driver subsystems are also an important part of the buck-boost power supply and are discussed below.

## *3.4 Switching Regulator IC*

A µA78S40 switching regulator IC was used to provide closed loop control of the pulse width modulated (PWM) signal to the switch of the buck-boost converter. From Figure 5 the basic functionality of the chip becomes apparent. A basic inverting comparator configuration is used to detect if the output voltage of the buck-boost converter is higher or lower than the reference [6]. An inverting configuration had to be used since the output voltage of the buck-boost converter is inverted. From the output of the comparator, the necessary PWM signal is generated to provide closed loop (output voltage) feedback. This chip uses an open collector Darlington pair arrangement for the PWM output. The PWM output of was used to switch a FET via a gate drive circuit. The internal bipolar junction transistor (BJT) could not be used due to this project's high current specifications. A 5V signal was used for the driver collector and switch collector to minimize power consumption. This resulted in a 0-3.5V PWM signal output to the gate drive circuit. The timing capacitor was selected so that the switching frequency was roughly 50kHz to minimize the inductor value.

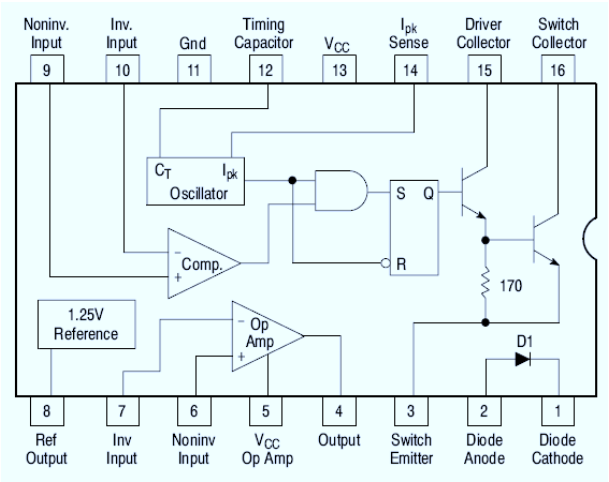


Figure 5: µA78S40 Functional Diagram

## *3.5 Gate Driver*

A gate driver acts as a voltage translator for the control signal and offers the control electronics isolation from the power electronics. The HCPL3120 optical isolator was used as a gate driver for a P-channel power MOSFET. A P-channel power MOSFET was used to simplify the gate drive design by eliminating the need for a floating gate drive circuit. Since a P-channel design was used, the logic output from the HCPL-3120 had to be inverted. Inverting this signal also ensured that the P-channel MOSFET would be "off" by default. Inversion of the signal was accomplished by using a P-channel MOSFET in a totem pole configuration with an N-Channel MOSFET (see Figure 9).

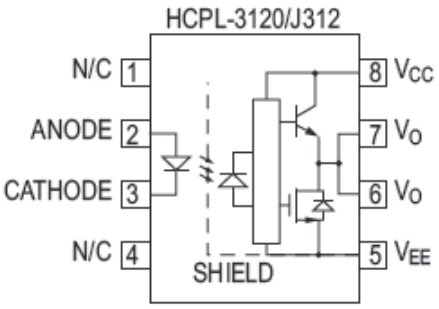


Figure 6: HCPL3120 Functional Diagram

Figure 6 shows the functional diagram of the HCPL3120 optical isolator. The recommended current for the anode was 16mA max. Using ohm's law with an input voltage of 5V, the necessary input resistance calculated had to be at least 312 ohms at the anode. Vcc was set equal to -15V with reference to Pos_Vin to ensure the P-channel MOSFET would switch quickly and be fully saturated. Vee was connected to the reference voltage Pos_Vin (see Figure 9). This

configuration forced the gate-to-source voltage (Vgs) of the P-channel MOSFET to be either 0V or -15V.

## *3.6 Lead Acid Fast Charge IC*

To control the battery charging characteristics and parameters, a lead acid fast charge IC was used. Essentially, this chip will control the voltage and current entering the battery as well as check for faults during the battery charging process. Possible faults could be that the battery thermistor temperature is not between 32 ºF and 106 ºF, a battery cell is open, a battery cell is shorted, a battery cell is faulty, current exceeds maximum rated current for the battery, or the battery is not present.

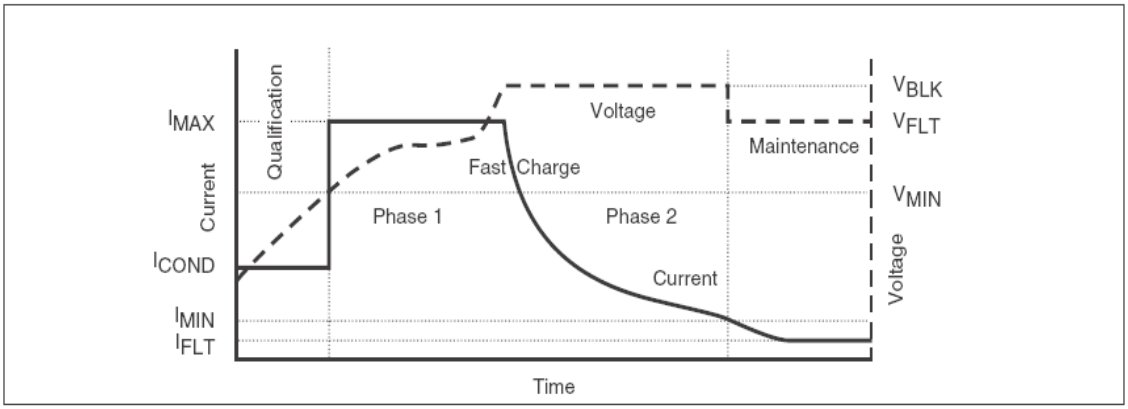


Figure 7: Two Step Voltage Charge Algorithm of BQ-2031 [7]

The voltage output of the buck-boost systems must be 14.2V+Vd so that after the voltage drop of the diode between the buck-boost system and the BQ2031 the voltage will be 14.2V. To charge lead-acid batteries, the two step voltage charge algorithm shown in Figure 7 is used. First, there is a qualification step that checks to make sure the faults listed above are not present. Next, the voltage across the battery terminals rises to the bulk charge voltage. The bulk charge voltage (Vblk in Figure 7) is then held constant until the defined minimum current is reached. This current is maintained and maintenance charging begins by changing the charging voltage to the specified float voltage (Vflt in Figure 7). To setup this chip for a lead acid battery to be charged in two-step voltage regulation, the Matlab code shown in Figures A-5 through A-7, Appendix A, was utilized. Figure A-8 shows the results of the calculations and the component values necessary to charge the stationary battery.

## *3.7 Stationary Battery*

The stationary battery will store renewable energy until power is needed to charge a mobile battery. Several different battery chemistries were considered for use as the stationary battery. A synopsis of the differences in battery chemistries is shown in Appendix A, Figure A-6. The stationary battery selected was an Optima D31T. It is a lead acid type to accommodate deep cycle discharging, trickle charging, and constant battery capacity throughout its lifetime

[8]. In addition, the battery is readily available and offers the best capacity for the price.

The battery specifications are 12V, 75Ah, with a bulk charge voltage specified as between 13.8 and 15.0 volts at 10A maximum. The maintenance charge voltage (Vflt) is between 13.2 and 13.8 volts. In addition, the temperature of the battery should remain below 125 °F [9]. When the battery capacity drops to 80%, it will be assumed the battery has reached the end of its life [10].

### *3.8 Mobile Battery Charger*

The mobile battery charger subsystem is similar to the stationary battery charger subsystem. However, the mobile battery charger will have the ability to switch modes. The mobile battery charger will accept power from the stationary battery and the (paralleled) stationary battery charger. The buck-boost for this system will need to regulate the voltage slightly higher to meet the specifications of the mobile battery discussed below. In addition, the BQ2031 configuration m-file in Figure A-5 will need to be re-run with the mobile battery specifications to determine the BQ2031 values.

The microcontroller will use analog to digital converters to read measurements from sensors in the mobile battery charger to display data to the user. The microcontroller will have the ability to switch from rapid charge and trickle charge via a digital output to the BQ2031. Since the mobile battery charger and microcontroller were not implemented there are no exact details on how this would be done.

### *3.9 Mobile Battery*

The mobile battery will be an electric car battery. For proof of concept, this project will use a Panasonic LC-RA1212P 12V lead-acid battery, used for the Gaucho. The rated capacity for this battery is 12V, 12Ah. The charging characteristics of this battery are the same as the stationary battery except the bulk charge voltage is between 14.5 to 14.9 volts and the maximum current is 4.8A. The specified float voltage is equal to 13.6 through 13.8 volts [11].

## 4. Simulations

After researching the basic structure of the buck-boost system, simulations in PSpice were conducted to ensure that the theory was sound and the topology selected would indeed work.

The first simulation included just the basic buck-boost topology using an N-channel MOSFET to do the switching with an ideal power source providing the gate signal. This permitted monitoring

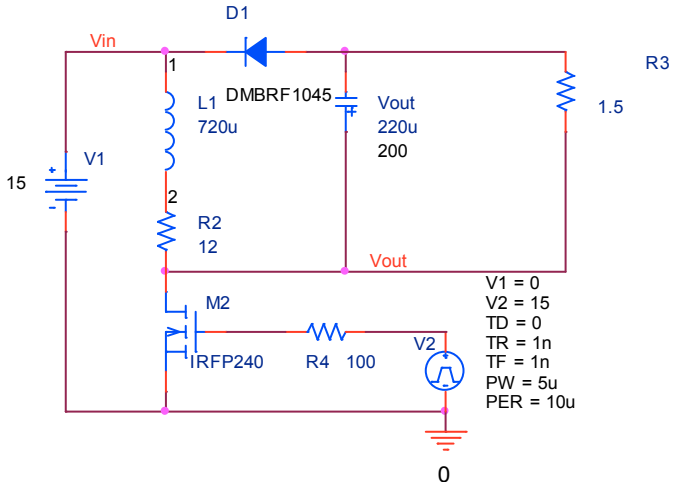


Figure 8: Buck-Boost Simulation Schematic

the output voltage to ensure the circuit would boost and buck as anticipated. Also, this ensured that the buck-boost converter would operate in continuous mode. After observing that the inductor current was indeed continuous and the output was as anticipated the gate drive circuitry was implemented. The components used in the Gate drive circuitry did not have models in PSpice so simulations were not implemented.

# 5. Implementation

After simulations were completed to ensure basic functionality, the system was implemented in hardware. The schematic in its entirety is located in Appendix C. The individual circuit diagram for each subsystem will be discussed below.

## *5.1 Buck-Boost*

The entire buck-boost schematic with feedback and gate drive circuitry is shown in figure 9. The simulated buck-boost schematic was modified slightly to be able to ground the output and use a low side driver configuration. In the final buck-boost circuit a P-channel MOSFET was used for switching, and an optical isolator driven by a -15V linear voltage regulator was used as a gate driver. Since the device was P-channel, the logic from the µA78s40 control chip was inverted to accommodate this change. The inversion was implemented using a P-channel and N-channel transistor configured such that when the input is high the output is low and vice versa. Snubber circuitry was added in the form of an RC circuit and a diode. The snubber circuitry ensures the MOSFET does not turn on and off too

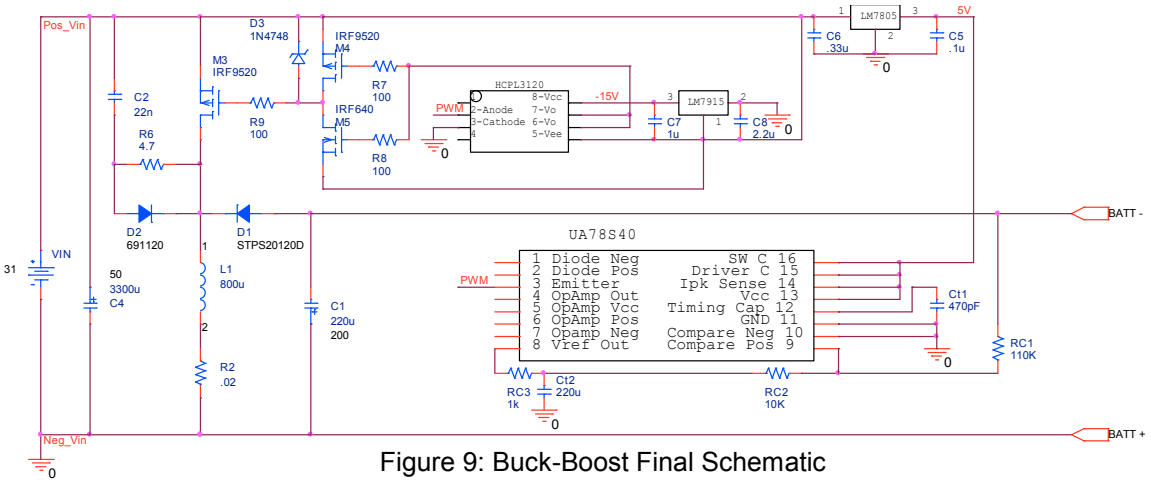


Figure 9: Buck-Boost Final Schematic

rapidly, damaging the MOSFET due to inductive voltage spikes. The comparator of the µA78s40 had the non-inverting input grounded to create a virtual ground at the inverting input. By doing so, the reference and output voltages could be compared by using a simple network of resistors. This is the inverting configuration of the µA78s40. By adjusting RC1 and RC2 in the schematic the output voltage can easily be adjusted. The output voltage is adjusted by the equation:

$$Vout = \frac{1.25 * RC1}{RC2 + RC3}$$

In system testing a trimming potentiometer was used in place of RC1 so that the output voltage could be varied according to different batteries. A low-pass filter was used on the reference voltage to remove noise so that the voltage could reliably be used to control the output. The µA78s40 was setup to run at 50 kHz as determined by the timing capacitor Ct1. A linear 5V regulator was used to provide power to the µA78s40 and ensured the control signal would be 0-3.5V consistently.

### *5.2 BQ2031*

Charging algorithms are handled using the BQ2031 fast-charge IC. The BQ2031 schematic was designed according to the recommended configuration in the datasheet. The schematic for the BQ2031 is shown in figure 10.

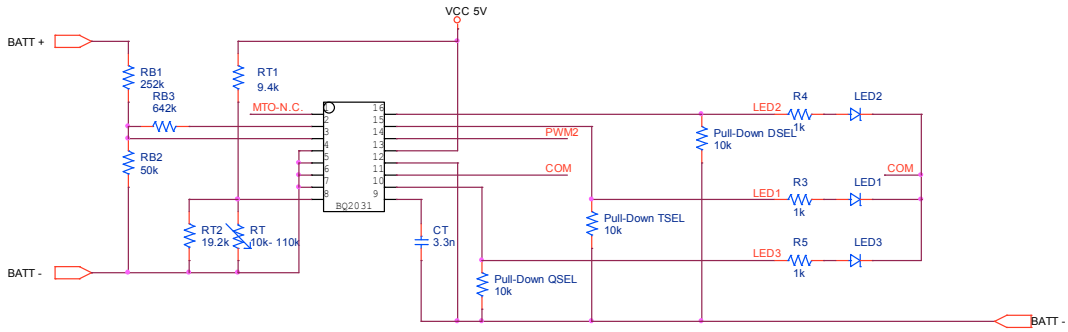


Figure 10: BQ2031 Final Schematic

The resistor network of RB1, RB2, and RB3 determines the voltage at which the battery will be charged. RT, RT1, and RT2 are used to set the temperature at which the battery will charge. MTO is the maximum time-out which has been left as an open circuit to maximize that parameter. CT sets the frequency at which the chip regulates the voltage. The LEDs show what state the charge cycle is in (i.e. float charge, constant current, constant voltage). The PWM output from the BQ2031 is used to drive a MOSFET which is connected in series to the positive battery terminal. The PWM keeps the battery from receiving too high of current (or rises too high in temperature) while the buck-boost regulates the proper voltage for the battery.

## 6. Data Sheet

Table 1 shows the voltages and currents for which the designed buck-boost system can handle reliably.

| Value | Min. | Typical | Max. | Units |
|---|---|---|---|---|
| Input Voltage ($V_{in}$) | 13.8 | 17 | 36 | Volts |
| Input Current ($I_{in}$) | - | 0.5 | 10 | Amps |
| Output Voltage($V_{out}$) | 0.125 | - | 25 | Volts |
| Output Power ($P_{out}$) | - | 0.77* $P_{in}$ | $P_{in}$ | Watts |

Table 1: Buck-Boost Specifications

The buck-boost system is capable of having the output voltage adjusted by means of a potentiometer. The potentiometer resistance ($R_p$) can change from 100Ω - 200kΩ and is varied by the equation:

$$Vout = \frac{1.25 * Rp}{10{,}000}$$

With this trimming potentiometer the maximum output allowable by the feedback circuit is 25V. It was calculated that the system has a 77% power efficiency, therefore 23% of the input power is dissipated in the circuitry.

The datasheet, power efficiency, and all results were determined under the charging conditions of 13.9V at 0.5A and with one P-channel MOSFET. This efficiency can be improved by paralleling multiple P-channel MOSFETs.

# 7. Analysis of Results

Upon implementing the buck-boost regulator in hardware the output voltage was able to be stabilized despite a widely varying input voltage. Figure 11 shows the output being regulated at 13.9V. There are some transitional spikes but these are so short they are negligible and could be eliminated with additional filtering. The final hardware design had constant output voltages with input voltages from 14V up to 35V. Also by adjusting the potentiometer on the µA78s40 the output voltage can be changed between 500mV to 25V in order to accommodate different batteries that may be connected to the system.

The voltage is regulated by the µA78s40 by creating a PWM to control the MOSFET that bucks or boosts the output voltage. This control signal is shown in Figure 12.

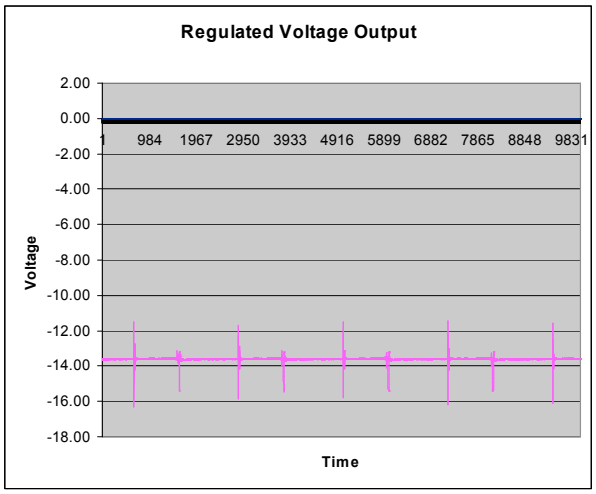


Figure 11: Regulated Output Voltage

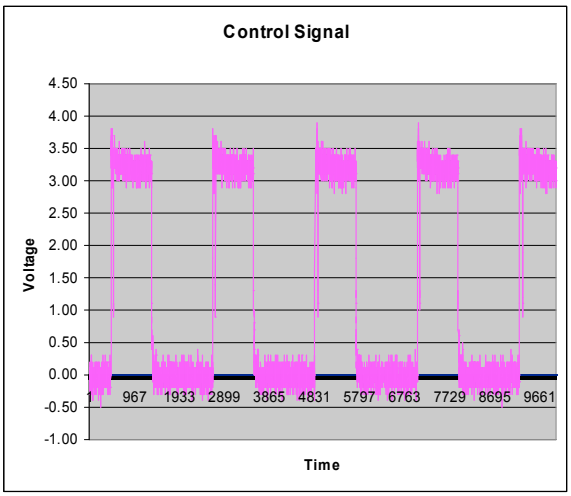


Figure 12: uA78s40 Output Control Signal

One of the most important things to check when verifying that the buck-boost system is working is that the current in the inductor is continuous. In figure 13 it is easy to see that the current in the inductor never reaches zero. The fact that it only gets within approximately 100mA from zero shows that the inductor is well sized for the switching frequency. The inductor current not reaching zero shows that the buck-boost is operating in continuous mode and the hardware design is sound.

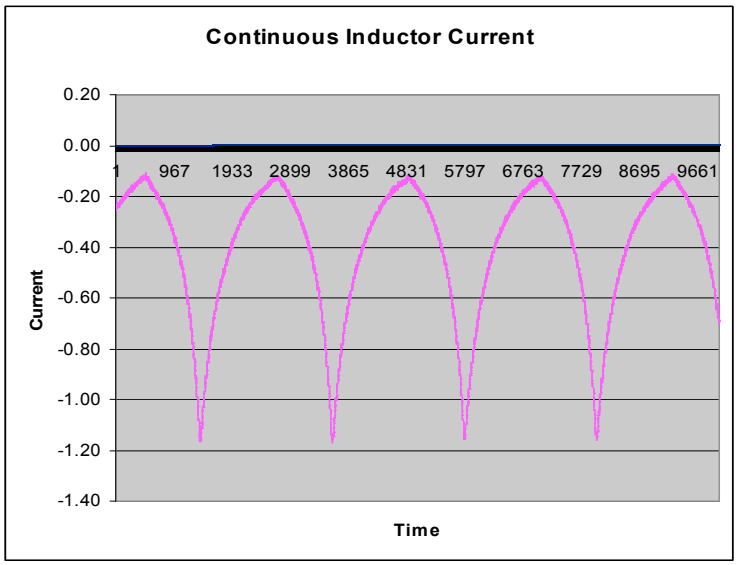


Figure 13: Continuous Inductor Current

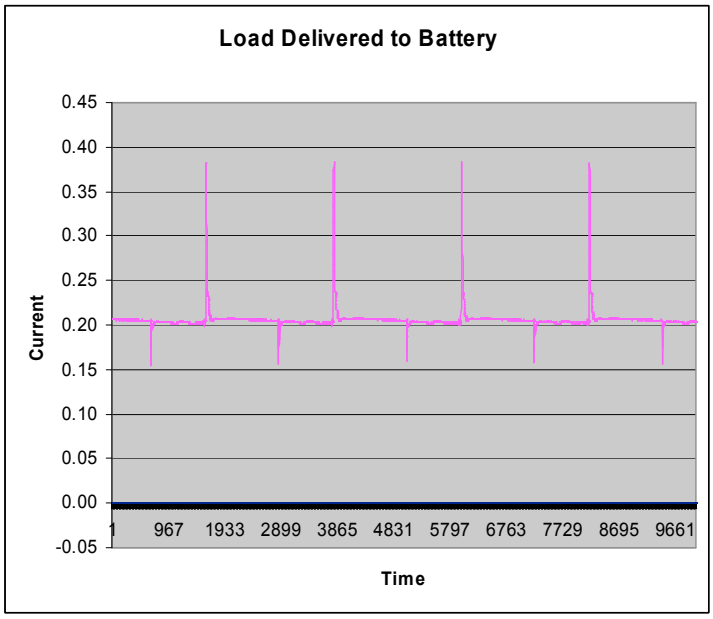


Figure 14: Current Delivered to Battery at 13.9V

Once the buck-boost system's operation had been verified, a basic application of charging was carried out. A small 5Ah battery was charged using the buck-boost converter for proof of concept. A diode was used to prevent the battery from discharging back into the buck-boost and an ammeter was used to monitor current into the battery as the battery was charged. By adjusting the potentiometer the current could be regulated by regulating the voltage to the battery terminals. Figure 14 shows current flowing into the battery thus charging the battery. Additional filtering will be needed to eliminate the high current spikes entering the battery.

# 8. Conclusions

The concept of a hybrid battery charger has been proven feasible by the results of this project. By achieving a switching power supply capable of regulating input voltages from 14V to over 35V, it becomes apparent that voltage regulation from solar panels or wind energy can easily be realized. A system capable of regulating an arbitrary voltage source at any desire output voltage allows for battery charging to be completed for any number of target batteries. To achieve a fully working system all that remains is a battery-to-battery charging system to charge the mobile battery from the stationary battery. The stationary battery charging can easily be handled with the buck-boost regulator already created. This system works as proof of concept of the hybrid charger, however more optimization would most likely be necessary for realistic applications.

# 9. Patents and Standards

The standards shown in Table 2 directly relate to electric vehicle charging systems, photovoltaic stand-alone systems, and safety. If the system were commercially marketed compliance to these standards would be mandatory.

| Relevant Standard | Description |
|---|---|
| IEC 62124 | Photovoltaic (PV) stand-alone systems Design verification [12] |
| IEC 61173 | Overvoltage Protection for Photovoltaic (PV) Power Generating Systems [12] |
| IEEE 1013 | Recommended Practice for Sizing Lead-Acid Batteries for Stand-Alone Photovoltaic (PV) Systems [12] |
| IEEE 485-1997 | IEEE Recommended Practice for Sizing Lead-Acid Batteries for Stationary Applications [13] |
| UL 2202 | Electric Vehicle Charging System Equipment [13] |
| UL 2231-1 | Personnel Protection Systems for Electric Vehicle (EV) Supply Circuits: General Requirements [13] |
| UL 2231-2 | Personnel Protection Systems for Electric Vehicle (EV) Supply Circuits: Particular Requirements for Protection Devices for Use in Charging Systems [13] |
| UL 2231-2 | Plugs, Receptacles and Couplers for Electric Vehicles [13] |

Table 2: Applicable Standards

The patents shown in Table 3 relate to systems similar to a hybrid battery charger for an electric vehicle. To avoid legal complications rights to the patents in the table may need to be investigated.

| Relevant Patents | Description |
|---|---|
| U.S. Patent #5646507 | Battery charger system [14] |
| U.S. Patent #6768285 | Power system for converting variable source power to constant load power [14] |
| U.S. Patent #4024448 | Electric vehicle battery charger [14] |
| U.S. Patent #5144218 | Device for determining the charge condition of a battery [14] |
| U.S. Patent #6204645 | Battery charging controller [14] |
| U.S. Patent #6677730 | Device and method for pulse charging a battery…[14] |

Table 3: Applicable Patents

# 10. References


[1] "Solar power insolation for U.S. major cities." Solar power can be a practical power source when using advanced photovoltaic equipment. 29 Nov. 2007 <http://solar4power.com/solar-power-insolation.html>.

[2] "Illinois Wind Maps." Energy Efficiency and Renwable Energy. 29 Nov. 2007 <www.eere.energy.gov/windandhydro/windpoweringamerica/images/windmaps/il_std800.jpg>.

[3] "Wind Powering America: Illinois Wind Maps." U.S. DOE Energy Efficiency and Renewable Energy (EERE) Home Page. 4 Dec. 2007 <http://www.eere.energy.gov/windandhydro/windpoweringamerica/where_is_wind_illinois.asp>.

[4] "AirX Specifications Datasheet." Southwest Windpower. 14 May 2008 <ee1.bradley.edu/projects/proj2008/lcc/pdf/wind_turbine_datasheet.pdf>.

[5] "Understanding Buck-Boost Power in Switchmode Power Supplies." Texas Instruments. 14 May 2008 <ee1.bradley.edu/projects/proj2008/lcc/pdf/TI_buck_boost.pdf>.

[6] "UA78S40 Universal Switching Regulator Subsystem Datasheet." ON Semiconductor. 14 Oct. 2008 <ee1.bradley.edu/projects/proj2008/lcc/pdf/ua78s40.pdf>.

[7] "U-511 Switch-Mode Power Conversion Using the BQ2031." Unitrode. 14 May 2008 < http://ee1.bradley.edu/projects/proj2008/lcc/pdf/bq2031_addition.pdf>.

[8] David, Linden, and Thomas Reddy. Handbook of Batteries. New York: McGraw-Hill Professional, 2002.

[9] "D31T Charging Specification Datasheet." Optima Batteries. 14 May 2008 <ee1.bradley.edu/projects/proj2008

[10] Kiehne, H.A.. Battery Technology Handbook, Second Edition (Electrical and Computer Engineering). Boca Raton: CRC, 2003.

[11] "Valve-Regulated Lead Acid Batteries: Individual Data Sheet LC-RA1212P." VLRA Batteries. 29 Nov. 2007

[12] "IEEE Revises Two Lead-Acid Battery Standards for Photovoltaic Systems - IEEE 937, IEEE 1013." IHS: The source for critical information and insight. 4 Dec. 2007 <electronics.ihs.com/news/ieee-photovoltaic-battery.htm>.

[13] "Search Engine for Standards." NSSN. 4 Dec. 2007 <http://www.nssn.org>.

[14] "Google Patents." Google. 4 Dec. 2007 <http://www.google.com/patents>.

# Appendix A: MATLAB Code

Editor - F:\Senior Project\Research\panelcalcsII.m

File Edit Text Cell Tools Debug Desktop Window Help

Stack: Base

```
%Blake Kennedy, Phil Thomas
%Advisor: Mr. Gutschlag
%Bradley University Spring 2008
%Algorithm for determining number of P.V. arrays needed to charge a
%battery and P.V. efficiency

clear all;
clear workspace;

solar_w=0.042;          %solar module width in meters
solar_l=0.125;          %solar module length in meters
cells=72;               %number of cells per module on P.V.
sun_hours_hi=4.475;     %max sun hours  %sun hour=Kilowatt-hrs/m²/day
sun_hours_lo=1.47;      %worst case sun hours
sun_hours_avg=3.76;     %average of high and low
battery_v=12;           %battery to charge voltage
battery_ah=12;          %battery to charge amp hour rating
batt_charge_eff=1.4;   %battery charing inefficiency
                        %= 1+(inefficiency percentage)
                        %(usually around 1.2 for lead acid)
                        %stationary battery(.2) + mobile battery(.2) =1.4
joules_max = 180000;    %maximum joules possible at maximum power rating
kW_max = joules_max/3600000;    %convert to kW
sun_density=1;          %Nominal Sun power Density defined in kW/m^2

mobile_wh=battery_v*battery_ah;         %capacity of battery in watt hours
mobile_j=mobile_wh*3600;                %capacity of battery in joules
solar_area=solar_w*solar_l*cells;       %calculate area of solar panel
solar_efficiency=kW_max/(solar_area*sun_density);
                                        %solar module efficiency
joules_hi=1e3*solar_area*solar_efficiency*3600;
                                        %calculate joules generates/module
if joules_hi>joules_max                 %check not over 54W rating
    joules_hi=joules_max;
end
joules_hi=joules_hi*sun_hours_hi;       %calculate no of Joules/module/day
joules_lo=1e3*solar_area*solar_efficiency*3600;
if joules_lo>joules_max
    joules_lo=joules_max;
end
joules_lo=joules_lo*sun_hours_lo;
joules_avg=1e3*solar_area*solar_efficiency*3600;
if joules_avg>joules_max
    joules_avg=joules_max;
end
joules_avg=joules_avg*sun_hours_avg;

number_solar_hi=(mobile_j*batt_charge_eff)/joules_hi
number_solar_lo=(mobile_j*batt_charge_eff)/joules_lo
number_solar_avg=(mobile_j*batt_charge_eff)/joules_avg
```

Figure A-1: Calculates the number of P.V arrays necessary and P.V. array efficiency

| Name | Value | Class |
|---|---|---|
| batt_charge_eff | 1.4 | double |
| battery_ah | 12 | double |
| battery_v | 12 | double |
| cells | 72 | double |
| joules_avg | 6.768e+005 | double |
| joules_hi | 8.055e+005 | double |
| joules_lo | 2.646e+005 | double |
| joules_max | 1.8e+005 | double |
| kW_max | 0.05 | double |
| mobile_j | 5.184e+005 | double |
| mobile_wh | 144 | double |
| number_solar_... | 1.0723 | double |
| number_solar_hi | 0.90101 | double |
| number_solar_lo | 2.7429 | double |
| solar_area | 0.378 | double |
| solar_efficiency | 0.13228 | double |
| solar_l | 0.125 | double |
| solar_w | 0.042 | double |
| sun_density | 1 | double |
| sun_hours_avg | 3.76 | double |
| sun_hours_hi | 4.475 | double |
| sun_hours_lo | 1.47 | double |

Figure A-2: Results of Figure A-1- Minimum Number of P.V. Arrays and Solar Efficiency

Editor - F:\Senior Project\Research\ComponentCalcs.m

File Edit Text Cell Tools Debug Desktop Window Help

```
%Blake Kennedy, Phil Thomas
%Bradley University
%Minimum Buck-Boost Component Sizes
%5/12/08

clear all;
clc;

%Variable Definitions
Vin_max=36;          %Maximum input voltage to buck-boost (V)
delta_Il=.1;         %Inductor ripple current (A)
Il=20;               %Maximum DC Inductor Current (A)
Rl=.1;               %Inductor DC Resistance (ohm)
D_min=20;            %Minimum duty cycle (%)
Fs=50000;            %Switching Frequency (Hz)
Rds_on=.1;           %.45 ohm paralleled multiple times (ohm)
Io_max=10;           %Maximum output current of buck-boost (A)
D_max=80;            %Maximum duty cycle (%)
delta_Vo=.5;         %Change in ripple voltage (V)

%Calculations
Vds_max=Il*Rds_on;  %Max Vds_off value of transistors (V)
Io_critical=delta_Il/2;%Min output I to maintain continous conduction (A)
Ton_max=(1/Fs)*(D_min/100);%Max transistor time on (s)
L_min=.5*((Vin_max-Vds_max-Rl)*Rl)*(Ton_max/(Il-delta_Il));
                     %Minimum inductance for buck-boost (H)
C_min=(Io_max*(D_max/100))/(Fs*delta_Vo);
                     %Minimum output capacitor size
ESR_max=delta_Vo/((Io_max/(1+(D_max/100)))+Io_critical);
                     %Maximum ESR with Capacitor
```

panelcalcsII.m | ComponentCalcs.m

script Ln 30 Col 48 OVR

Figure A-3: Calculates the minimum requirements of components in the buck-boost power stage

| Name | Value | Class |
|---|---|---|
| C_min | 0.00032 | double |
| D_max | 80 | double |
| D_min | 20 | double |
| ESR_max | 0.089197 | double |
| Fs | 50000 | double |
| Il | 20 | double |
| Io_critical | 0.05 | double |
| Io_max | 10 | double |
| L_min | 3.407e-007 | double |
| Rds_on | 0.1 | double |
| Rl | 0.1 | double |
| Ton_max | 4e-006 | double |
| Vds_max | 2 | double |
| Vin_max | 36 | double |
| delta_Il | 0.1 | double |
| delta_Vo | 0.5 | double |

Figure A-4: Results of Figure A-3- Minimum Component Requirements for Buck-Boost Converter

```
%BQ2031 Configuration for Lead Acid Battery Charging
%Equations from Unitrode BQ2031 Suppliment

%BQ2031 Defined Parameters
%Co=100uF;  %From suppliment
Cells=6;    %define number of cells in battery
Vflt=2.216;  %define float voltage for trickle charging battery
Vblk=2.36;  %define bulk charge voltage for charging battery per cell
Imax=10;    %define maximum current battery can take while charging
Imin=1;     %define minimum current battery can take while bulk charging
RB2=50e3;   %define value for RB2 (arbitrary- 50k recommended)
            %maintains charging voltage
Fs=30000;      %define switching frequecy in KHz
Vinmax=36;  %Define maximum input voltage
Vinmin=12;  %Define minimum input voltage
Ci=.000001; %Current Gain stability capacitor
            %Visually inspect Figure(1) and Figure(2)to ensure:
Ri=.0025;   %Internal Battery Resistance
Ah=75;  %Capacity of Battery in Ah
TCO=106;    %define high temperature to stop charging at (degrees F)
TCO=32;    %define low temperature to stop charging at (degrees F)

%"The gain and phase characteristics of the OTA and associated
%circuitry must be adjusted to meet the following
%three criteria for loop stability:
%1. Total open-loop gain (IL(s) and VL(s) above) must
%be forced to 0dB at a crossover frequency (FC) equal
%to at least 1/6 the switching frequency (FS).
%2. The phase of the total open-loop gain at FC must be
%at least 45 degress less than 180 degrees."


%BQ2031 Calculations
RB1=(((Cells*Vflt)/2.2)-1)*RB2;             %RB1 maintains charging voltage
RB3=2.2*RB1*RB2/((Cells*Vblk*RB2)-(2.2*(RB2+RB1)));
                                           %RB3 maintains charging voltage
Rsns=(.250/Imax);                          %current sense for shutoff

TCOK=((TCO-32.)/1.8)+273.15;               %TCO in Kelvin
```

Figure A-5: Configuration File for BQ2031 Part 1 of 3

```
40 -  TCOK=TCOK^-1%use with Fig 22.1 in notebook to find resistance Rtco
41            %relates to about 10.5k ohms
42
43 -  TCO=85;    %define temperature to resume charging after temp fault(degrees F)
44 -  TCOK=((TCO-32.)/1.8)+273.15;              %TCO in Kelvin
45 -  TCOK=TCOK^-1%use with Fig 22.1 in notebook to find resistance Rhtf
46            %relates to about 12k ohms
47
48 -  TCOK=((TCO-32.)/1.8)+273.15;              %TCO in Kelvin
49 -  TCOK=TCOK^-1%use with Fig 22.1 in notebook to find resistance Rtco
50            %relates to about 110k ohms
51
52 -  Cpwm=0.0001/Fs;    %Cpwm is defined in F
53
54    %Current Gain Stability
55 -  num=[0 0.47*Vinmax*105];
56 -  den=[250000*Ci 1];
57 -  figure(1)
58 -  w = [0.1: 0.1: 30000];
59 -  bode(num,den,w)
60 -  title('Current Loop Gain Transfer Function');
61 -  grid on
62
63    %Voltage Gain Stability
64 -  D=((1/RB2)+(1/RB3))^(-1)/(((1/RB2)+(1/RB3))^(-1)+RB1);
65    %Cf=1/(2*3.14*RB1*200);  %Assumes fz1=200Hz from Figure 9 in suppliment
66    %Cv=((1/(2*5*3.14))-(1/(2*3.14*200)))/(2.5*10^5);
67                          %Assumes fp1=5Hz from Figure 9 in suppliment
68                          %Assumes fz2=200Hz from Figure 9 in suppliment
69    %Rv=1/(2*3.14*Cv*200);   %Assumes fz2=200Hz from Figure 9 in suppliment
70
71
72
73 -  L=(Cells*Vblk*0.5)/(Fs*2*Imin);
74
75 -  Cb=100*Ah;
76 -  fzo=1/(2*3.14*Ri*Cb);
77 -  fpo=1/(2*3.14*(L*Cb)^0.5);
78 -  fz1=fpo/2;
```

Figure A-6: Configuration File for BQ2031 Part 2 of 3

```
fz2=fpo/2;

Cf=(1/(2*3.14*RB1*fz1));
fp2=1/(2*3.14*D*RB1*Cf);
Ro=Cells*(Vblk/Imax);
wo=1/(L*Cb)^.5;

Fc=Fs/20
num=[250000*Cb*.47*Vinmax .47*Vinmax];
den=[(1/wo)^2 ((Ri*Cb)+(L/Ro)) 1];
w = [0.1: 0.1: 100000];
figure(2)
bode(num,den,w)
title('G(s)');
grid on

%G(Fc) is taken from Figure 3 to find A(fp2)
%A(fp2)= solve(20*log(1/x)=G(Fc)
%where G(Fc) is the gain of Figure 3 (G(s)) at Fc converted to decimal
%Rv=(A(fp2)*2.5*10^5)/(A(fp2)-(105*D));

Rv=(178.8e-9*2.5*10^5)/(178.8e-9-(105*D));
Cv=1/(2*3.14*Rv*fz2);
Ci=1/(2*3.14*(2.5*10^5)*(fpo/2));



num=[105*Cv*D*RB1*Rv 105*Cf*D*RB1+105*Cv*Rv 105*D];
den=[Cv*Cf*D*RB1*Rv+250000*Cv*Cf*D*RB1 Cf*D*RB1+Cv*Rv+250000*Cv 1];
figure(3)
w = [0.1: 0.1: 100000];
bode(num,den,w)
title('A(s)');
grid on
```

Figure A-7: Configuration File for BQ2031 Part 3 of 3

| Name | Value | Class |
|---|---|---|
| Ah | 75 | double |
| Cb | 7500 | double |
| Cells | 6 | double |
| Cf | 7.4608e-006 | double |
| Ci | 7.526e-006 | double |
| Cpwm | 3.3333e-009 | double |
| Cv | -686.66 | double |
| D | 0.15537 | double |
| Fc | 1500 | double |
| Fs | 30000 | double |
| Imax | 10 | double |
| Imin | 1 | double |
| L | 0.000118 | double |
| RB1 | 2.5218e+005 | double |
| RB2 | 50000 | double |
| RB3 | 6.4213e+005 | double |
| Ri | 0.0025 | double |
| Ro | 1.416 | double |
| Rsns | 0.025 | double |
| Rv | -0.0027401 | double |
| TCO | 85 | double |
| TCOK | 0.0033048 | double |
| Vblk | 2.36 | double |
| Vflt | 2.216 | double |
| Vinmax | 36 | double |
| Vinmin | 12 | double |
| den | [-5.0182e+007 -1.7... | double |
| fp2 | 0.54473 | double |
| fpo | 0.16927 | double |
| fz1 | 0.084633 | double |
| fz2 | 0.084633 | double |
| fzo | 0.0084926 | double |
| num | [7.7404e+006 228.2... | double |
| w | <1x1000000 double> | double |
| wo | 1.063 | double |

Figure A-5: BQ2031 Configuration File Results

# Appendix B: Battery Comparison

| | Optima Lead Acid | Li-Ion | Ni-CD | Ni-MH | Sealed Lead Acid |
|---|---|---|---|---|---|
| Temperature Range (C) | 130 to -30 | 50 to -20 | 45 to -40 | 50 to -20 | 60 to -40 |
| Calendar Life (years) | ? | 2 to 5 | 2 to 5 | 2 to 5 | 2 to 8 |
| Max Charge Cycles | 300+ | 1000+ | 300 to 700 | 300 to 600 | 250 to 500 |
| Discharge Profile | Flat | Slope | Flat | Flat | Flat |
| Self Discharge Rate @ 20C (% /mo) | Very Low | 2 | 15 to 20 | 15 to 25 | 4 to 8 |
| Memory Effect | No | No | Yes | Yes | No |
| Ability to Trickle Charge | Yes | No | Yes | Yes | Yes |
| Charging Characteristic | | 2 stage | | | |
| Deep Discharge | Yes | Yes | Yes | Yes | No |
| Relatively Quick Charge | Yes | Yes | Yes | Yes | No |
| Constant Voltage Or Current Charge | Voltage | Voltage | Current | Current | Voltage |
| Relative Expense/ Capacity | Cheap | Expensive | Moderate | Moderate | Cheap |
| Approx Expense (dollars) | 150 | < 600 | 300 | 350 | 80 |

Figure B-1: Battery Chemistry Summary

# Appendix C: Final Schematic

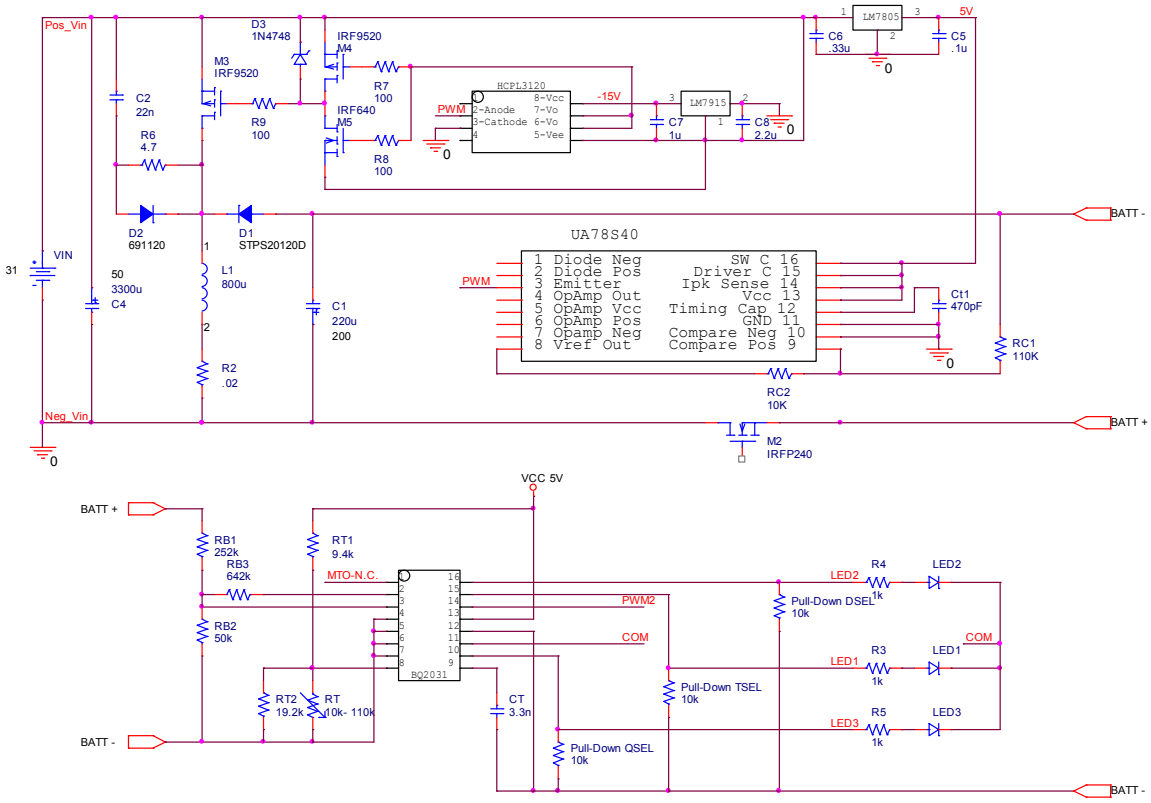


Figure C-1: Final Schematic